

See discussions, stats, and author profiles for this publication at: <https://www.researchgate.net/publication/282151829>

# Hernandez DiamRelMat(15) GR on Pt Au by MBE C-source

Data · September 2015

CITATIONS

0

READS

80

5 authors, including:



**Irene Hernández-Rodríguez**

Instituto de Ciencia de Materiales de Madrid

10 PUBLICATIONS 30 CITATIONS

[SEE PROFILE](#)



**Jorge M. García**

Spanish National Research Council

195 PUBLICATIONS 7,100 CITATIONS

[SEE PROFILE](#)



**Jose Angel Martin Gago**

Spanish National Research Council

220 PUBLICATIONS 3,635 CITATIONS

[SEE PROFILE](#)



**Pedro L. De Andres**

Spanish National Research Council

131 PUBLICATIONS 2,264 CITATIONS

[SEE PROFILE](#)

Some of the authors of this publication are also working on these related projects:



Ballistic Electron Emission Microscopy [View project](#)



Electrodynamics on Thin Films [View project](#)



# Graphene growth on Pt(111) and Au(111) using a MBE carbon solid-source

Irene Hernández-Rodríguez <sup>a</sup>, Jorge M. García <sup>b,c</sup>, José A. Martín-Gago <sup>a</sup>, Pedro L. de Andrés <sup>a</sup>, Javier Méndez <sup>a,\*</sup>

<sup>a</sup> Instituto de Ciencia de Materiales de Madrid, ICMM-CSIC, 28049 Madrid, Spain

<sup>b</sup> Instituto de Microelectrónica de Madrid, IMM-CNM, CSIC, 28760 Madrid, Spain

<sup>c</sup> Campus de Excelencia Internacional, UAM+CSIC, Madrid, Spain

## ARTICLE INFO

### Article history:

Received 27 November 2014

Received in revised form 2 March 2015

Accepted 3 March 2015

Available online 5 March 2015

### Keywords:

Graphene

Graphene on metals

MBE carbon source

Scanning tunneling microscopy STM

## ABSTRACT

In this work we present a Molecular Beam Epitaxy (MBE) growth method to obtain graphene on noble metals using evaporation of carbon atoms from a carbon solid-source in ultra-high vacuum conditions. We have synthesized graphene (G) on different metal surfaces: from a well studied substrate as platinum, to a substrate where it can only be formed using innovative methods, as is the case of gold. For the characterization of the graphene layers we have used in situ surface science techniques as low energy electron diffraction (LEED), auger electron spectroscopy (AES) and scanning tunneling microscopy (STM).

One of the main advantages of our methodology is that low surface temperatures are required to form graphene. Thus, by annealing Pt(111) and Au(111) substrates up to 650 °C and 550 °C respectively during carbon evaporation, we have obtained the characteristic LEED diagrams commonly attributed to graphene on these surfaces. STM results further prove the formation of graphene. For the case of G on Pt(111), STM images show a long range ordering associated with moiré patterns that correspond to a monolayer of graphene on (111) platinum surface. On the other hand, G/Au(111) STM results reveal the formation of dendritic islands pinned to atomic step edges. This method opens up new possibilities for the formation of graphene on many different substrates with potential technological applications.

© 2015 Elsevier B.V. All rights reserved.

## 1. Introduction

Graphene has become an important prototype material with interesting technological applications and properties [1]. This 2D honeycomb structure composed of a single layer of carbon atoms presents striking properties. Among others, it has a high electrical and high thermal conductivity, and a strong mechanical strength. The combination of these properties in one single material has boosted a plethora of promising practical applications such as nanocomposites, sensors, energy storage devices, and transparent conducting films.

Preparation methods of graphene greatly vary from mechanical exfoliation of graphite [2] (widely used in research laboratories), graphite oxidation [3] (using wet chemistry techniques), to Chemical Vapor Deposition [4,5] (CVD) (easily up-scalable for industrial applications). Recently, the use of a mixer has shown the possibility to obtain graphene in large quantities from a non-expensive mechanical method [6]. However, for the case of CVD graphene synthesis by decomposition of organic precursors, the catalytic properties of metallic substrates play a fundamental role during cracking processes of C–H bonds. A synthesis method allowing the growth of high quality large-area graphene with

possibilities of becoming a transfer-free process will represent a great advance in fundamental and applied research, and could have great-unforeseen technological impact. A detailed atomistic understanding of the synthesis mechanisms of graphene is a keystone towards a Graphene On Insulator (GOI) large-area technology development.

The possibility of growing graphene by means of a MBE-inspired method will allow the use of many in situ surface science characterization techniques that will greatly help understanding the formation mechanisms of graphene [7,8]. In this work we demonstrate, using these tools, the successful growth of graphene on two noble metal surfaces: Pt (111) and Au (111). We show that this methodology requires a much lower substrate temperature annealing than other reported methods [9–12].

One of the main advantages of MBE growth is the possibility to precisely control parameters such as growth time, chamber pressure or substrate temperature. Up to now, the direct deposition of carbon atoms on a substrate using an MBE has been rarely reported [13–18], and quality of graphene has been often evaluated using XPS or ex situ Raman spectroscopy. On the other hand, low-temperature MBE growth of graphene on Copper has been reported by Meng Yu-Ling et al. [13]. Their work shows atomic-resolution STM images of graphene on Copper between RT to 300 °C, demonstrating the capacity of this method to form graphene at low temperatures. In this paper we show STM images with atomic resolution of the characteristic moiré of G/Pt(111). For

\* Corresponding author.

E-mail address: [jmendez@icmm.csic.es](mailto:jmendez@icmm.csic.es) (J. Méndez).

the case of G/Au(111), STM images reveal the formation of dendritic islands pinned to the atomic step edges.

Up to date, most published works report methods for growing graphene that use too high temperatures to be compatible with other processing techniques. For example, a single-crystal of gold needs to be annealed to temperatures close to the roughening transition, which is usually 0.75 of the melting temperature, i.e. 800 °C. Thus, during graphene formation by decomposition of irradiated ethylene [9] the substrate has to be annealed up to 950 °C, a temperature at which the gold crystal can easily become amorphous. Another example is the molecular decomposition of polycyclic aromatic precursors [10], where the substrate has to be at 727 °C to achieve graphene formation. Another method to synthesize graphene using an electron beam evaporator has also been reported [11,12] using a substrate temperature of 950 °C. On the other hand, the growth of graphene by MBE carbon solid-source proposed in this work requires a temperature around 550 °C–650 °C, a significant reduction in temperature compared to previous methods.

Additionally, the formation of carbonaceous deposits on Pt(111) surfaces and Pt nanoparticles has been studied from a theoretical point of view using models and density-functional calculations [19].

The object of this work is to probe the efficiency for growing graphene on different substrates of the methodology based on a MBE carbon source. This solid carbon source has two main advantages: (i) to obtain graphene on different substrates independently of the catalytic properties of the sample; and (ii) to significantly reduce the substrate temperature with respect to other methods.

## 2. Experimental

The experiments were performed in an Ultra High Vacuum (UHV) chamber with surface preparation and characterization techniques: ion sputtering, LEED, AES, and STM. The chamber also includes a homemade carbon source. It consists of two tantalum bars connected through a glassy carbon filament (Fig. 1a). By passing through the glassy carbon filament a DC current of 14 A (7.9 V, 110 W) reaches evaporation conditions at a temperature of 2000 °C, as measured with an infrared optical pyrometer. The deposition rate of carbon on the substrate estimated from STM measurements is approximately  $3 \times 10^{-4}$  ML/s. The substrate, placed at 20 mm in front of the carbon source, is annealed at 550 °C in the case of Au(111) and 650 °C for Pt(111). The evaporation of carbon takes place during 30 min, which corresponds to a coverage close to half of a monolayer.

Before growth, the substrates were cleaned by cycles of Ar<sup>+</sup> sputtering and annealing. Both crystals were Ar<sup>+</sup> sputtered at 1.5 KeV. Pt(111) was annealed up to 950 °C while the gold substrate was annealed up to 450 °C. Cycles are repeated until the LEED

pattern shows sharp spots and the Carbon peak measured by AES is not detectable.

Experiments were performed at a base pressure of  $1 \cdot 10^{-10}$  mbar, however, during evaporation the pressure reaches up to  $1 \cdot 10^{-8}$  mbar. We have measured the growth of graphene with LEED and STM at room temperature in the same chamber on the two mentioned substrates. The STM images were obtained using an Omicron VT-STM operated with Nanotec's WSxM [20] software and electronics.

## 3. Results and discussion

The LEED pattern in Fig. 2a shows the characteristic graphene ring obtained after evaporation of 0.5 ML of carbon on a Pt (111) surface at 650 °C. The 2D lattice constant of the rhombohedral unit cell of graphene is 2.46 Å, while the one for platinum is 2.75 Å. Therefore, the spots of graphene appear at a larger distance in the diffraction pattern than the platinum spots. On the other hand, the presence of a ring corresponding to graphene indicates that there are graphene patches orientated in all directions on the substrate. The ring is discontinuous, brighter around 19° with the platinum spots, indicating that this is the most common orientation of graphene. This result is in good agreement with the geometric model reported by Merino et al. [21].

STM shows extended regions of surface covered by graphene [22,23] in a surface morphology similar to that reported by the thermal decomposition of hydrocarbons [10,24]. We have analyzed regions up to  $1 \mu\text{m} \times 1 \mu\text{m}$  and we have concluded that graphene coverage is about 50% of the surface. STM images show several moiré patterns separated by domain boundaries that appear as bright features together with a dark seam line (Fig. 2b). Some 3D nucleated protrusions can also be observed and are tentatively attributed to amorphous carbon.

Atomic resolution images (Fig. 2c) clearly show a moiré pattern obtained at low bias voltages and tunnel currents ( $V = -35.7$  mV,  $I = 0.04$  nA). The moiré pattern shown in Fig. 2c can be interpreted according to the model shown in Fig. 2d where the top layer of graphene is rotated 2° with respect to the underlying Pt(111) surface. The angle between carbon and the moiré bumps is of 16.5°, with a periodicity between bumps of 2.1 nm.

In addition, we have successfully grown graphene on Au(111) using the experimental protocol. After exposing the gold sample at 550 °C to the MBE carbon source for 30 min, we obtain the LEED pattern observed in Fig. 3a. It shows graphene diffraction spots around the hexagonal Au(111) pattern, corresponding to lattice parameters of 2.46 Å and 2.88 Å, respectively. The graphene spots are elongated and are rotated zero and thirty degrees with respect to the gold spots. This result indicates that, on the surface of Au(111), graphene is either aligned with the substrate or with carbon atoms along the (110) direction, respectively. The observed LEED diagram can be described by arrangements of graphene rotated 0° and 30° with respect to the Au(111). From the hard ball model shown in Fig. 2d we deduce that the Moiré patterns correspond to  $7 \times 7$  and  $3 \times 3$  structures, respectively.

STM images for graphene on Au(111) show dendritic island growing at both sides of gold step edges or pinned by defects (Fig. 3b). In many cases graphene can be clearly distinguished by analyzing STM current images (Fig. 3c) in which the graphene covered areas correspond to dark regions, while bright areas correspond to uncovered gold. A closer view on graphene permits us to recognize several moirés marked with red arrows in Fig. 3d, in good agreement with other works [11,25]. The presence of moiré patterns confirms that the dendritic islands correspond to graphene on gold. The Au(111) herringbone reconstruction (blue arrows in Fig. 3d) can be used to infer the orientation of the moiré with respect to the crystallographic directions of gold. Thus, the middle graphene patch in Fig. 3d is oriented along the gold atom direction. This alignment is in agreement with what is observed in the LEED diagram (spots at 0°).

STM topographic images of graphene on gold are usually revealed as depressions. This fact can be related to a smaller electrical conductivity

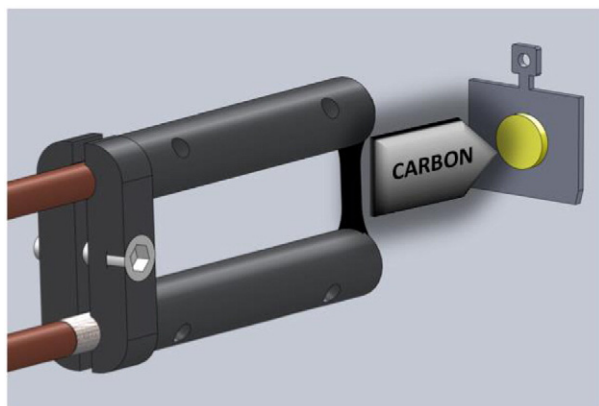
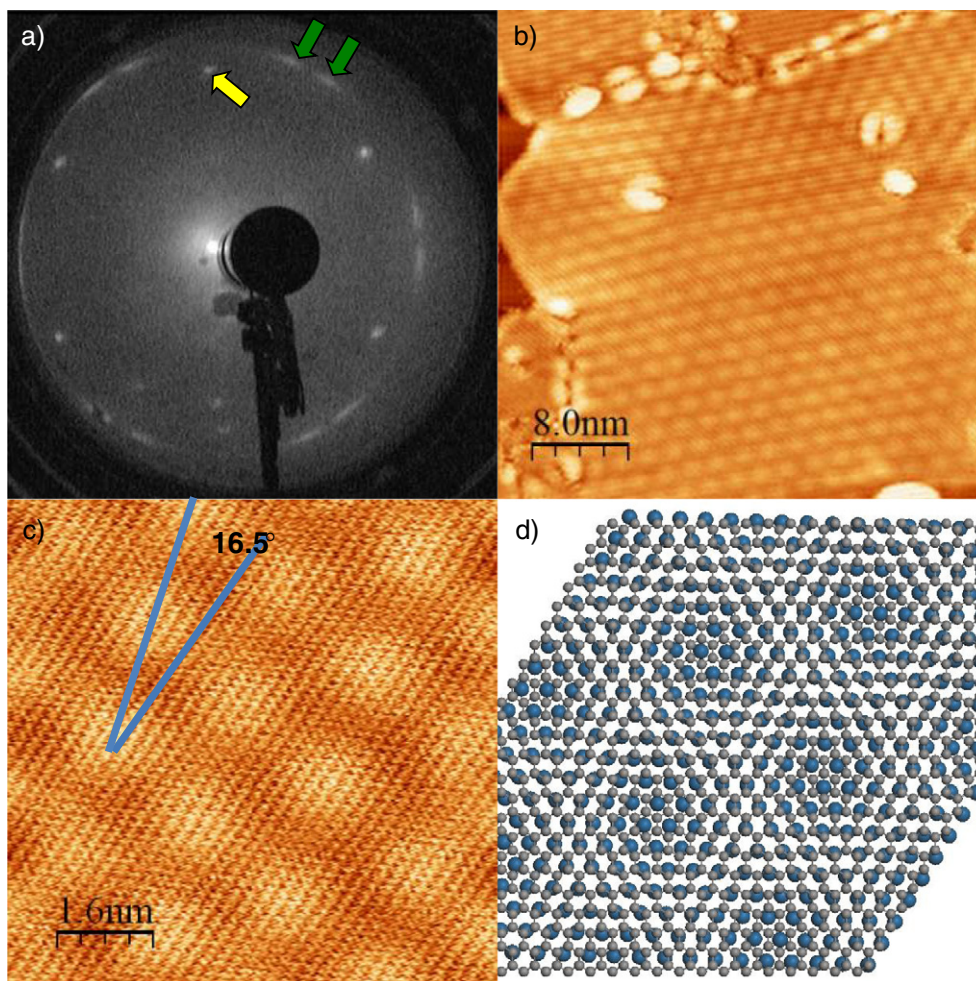


Fig. 1. Scheme of the homemade carbon source consisting on two tantalum bars connected through a glassy carbon filament, system followed for graphene growth.





**Fig. 2.** a) LEED image taken at 57.4 V on platinum after graphene growth. Spots related to Pt(111) form the characteristic hexagonal pattern (yellow arrow) surrounded by a discontinuous ring (green arrows) corresponding to graphene; b) STM picture showing several of the characteristic graphene moirés separated by grain boundaries visualized as brighter areas. Size: 65 nm  $\times$  65 nm,  $V = -35.7$  mV,  $I = 0.04$  nA; c) Atomic resolution image of graphene on Platinum. The angle between the direction of the moiré bumps and the atoms lines is 16.5°. Size 8 nm  $\times$  8 nm,  $V = -3507$  mV,  $I = 0.04$  nA. d) Hard ball model for the moiré obtained by rotating 2° between graphene and platinum layers. 2c. Gray (blue) spheres represent carbon (platinum) atoms.

in the layer of graphene on gold than the gold itself. It could also be related to adsorbates on the STM tip that will induce a reversed contrast [26]. Fig. 3e is a schematic representation of a constant-current topographic scanning profile over the sample. Over graphene regions, the STM tip must approach the surface to maintain a constant tunneling current. This produces an inverted contrast on the apparent topography: graphene appears dark (depressions) and bare gold appears bright. In comparison to G/Au(111), uncovered gold regions are visualized by STM as noisier patches, which may be due to the presence on the surface of fast diffusing carbon species, as it has been previously reported for organic molecules on gold [27].

In order to obtain the minimum temperature for graphene formation, and to check the difference between both materials, we have also performed carbon evaporation on platinum at 550 °C. In this case, no order graphene layer has been obtained but unordered carbonaceous growth. This fact indicates that the minimum temperature to form graphene is substrate dependent. We suggest that the important parameter is the carbon diffusion barrier. We have calculated [28] the diffusion barriers for carbon on gold and for carbon on platinum finding that it is lower for gold by 61 meV. Therefore, to achieve the diffusion rate necessary to form graphene, the temperature of the platinum substrate has to be increased by 60 °C calculations, in agreement with the 100 °C temperature increase needed to observe ordered graphene on platinum.

The difference in the aspect of the graphene grown on both substrates, i.e. dendritic growth on gold versus extended moiré on platinum, is related to a second process: the carbon diffusion at the graphene island's perimeter. This process is similar on both substrates and it is dominated by the carbon–carbon interaction. In this case, the higher temperature of the platinum substrate makes the graphene to be more ordered, where the graphene on gold keeps the shapes of the nucleation process.

#### 4. Conclusion

Graphene can be successfully grown using a carbon solid-source on transition metal surfaces, including low reactive ones, as gold. This method represents an important improvement over others since MBE allows us to obtain graphene keeping the substrate at lower temperatures. We have tested our methodology using Pt(111) and Au(111) surfaces. Crystallinity and morphology of graphene on the metals have been checked using LEED and STM techniques. We show that graphene grows on Pt(111) forming several moiré patterns on atomically flat areas, while graphene on Au(111) grows in dendritic islands pinned by steps or substrate defects. These differences can be attributed to the dynamic of the processes occurring during graphene formation, mainly carbon diffusion on the substrates and at the edges of the graphene islands.

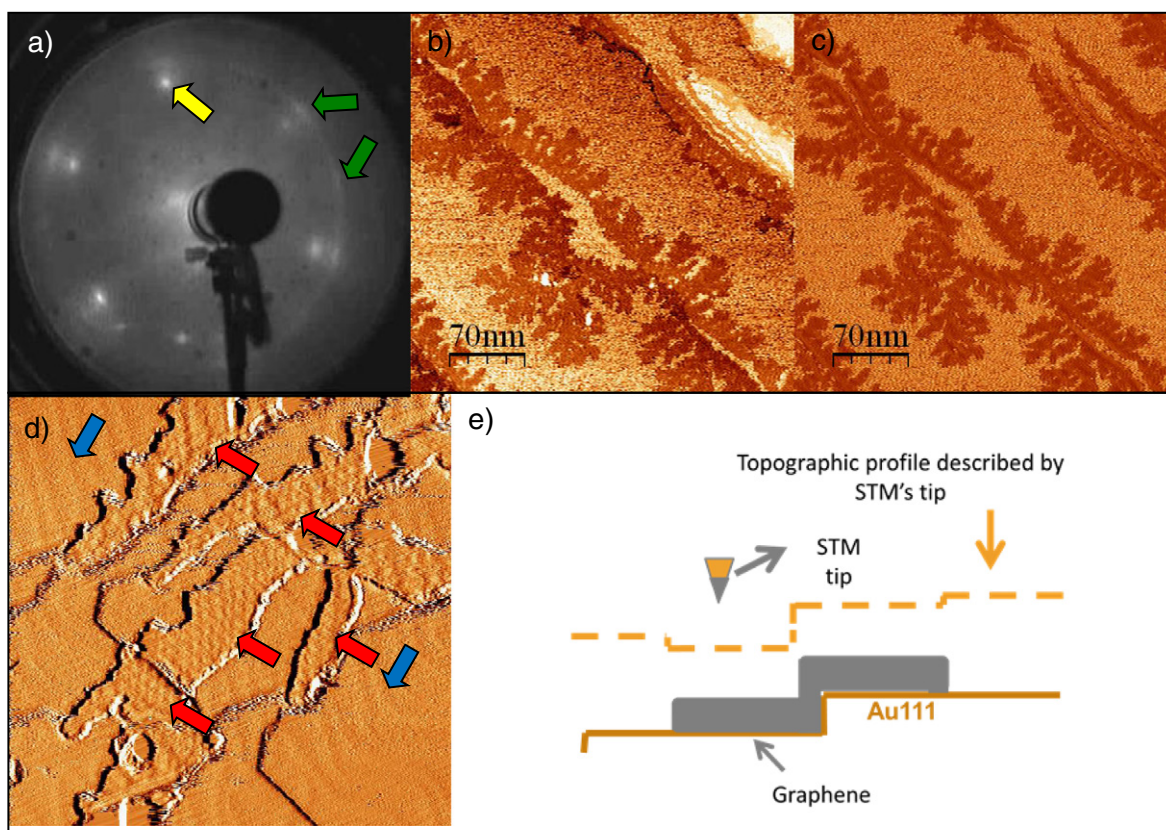


**Fig. 3.** a) Picture of the LEED pattern of gold after graphene growth. Spots associated with Au(111) form a hexagonal pattern (yellow arrow) which is surrounded by a characteristic graphene diffraction pattern. The graphene diffraction spots are brighter at  $0^\circ$  and  $30^\circ$  (green arrows). Image obtained using a primary electron beam energy of 55.1 eV; b) STM Topographic and c) STM current images showing graphene growth on Au(111). Graphene areas are clearly distinguished at the current image, as substrate appears noisy and lighter. Size:  $350 \text{ nm} \times 350 \text{ nm}$ ;  $I = 4 \text{ pA}$ ;  $V = -1241 \text{ mV}$ ; d) STM image in derivative mode showing graphene areas as dendritic branches (red arrows) with several types of moirés. The gold herringbone reconstruction is viewed on some of the uncovered areas (blue arrows). Size of the image:  $67 \text{ nm} \times 67 \text{ nm}$ ;  $V = -107.8 \text{ mV}$ ;  $I = 1 \text{ pA}$ ; e) Scheme showing the topographic constant-current profile described by STM tip. Tip gets closer over the graphene islands, even when the tip-surface distance is reduced, inducing a reverse effect and making the graphene to be viewed as depressions.

### Prime novelty statement

This paper shows for the first time the growth of graphene from a MBE carbon source on platinum and gold single crystals. We prove using LEED and STM characterization techniques that graphene is formed on these substrates. The substrate temperature during the process is much lower than in other methods.

### Acknowledgments

The research leading to these results has received funding from Spanish Projects MAT2011-26534, MAT2014-54231 and AIC-B-2011-0806, and from European Union Seventh Framework Program under grant agreement no. 604391 Graphene Flagship.

### References

- [1] A.H. Castro Neto, F. Guinea, N.M.R. Peres, K.S. Novoselov, A.K. Geim, The electronic properties of graphene, *Rev. Mod. Phys.* 81 (2009) 109–162.
- [2] A.K. Geim, K.S. Novoselov, The rise of graphene, *Nat. Mater.* 6 (2007) 183–191.
- [3] S. Stankovich, D.A. Dikin, R.D. Piner, K.A. Kohlhaas, A. Kleinhammes, Y. Jia, Y. Wu, S.T. Nguyen, R.S. Ruoff, Synthesis of graphene-based nanosheets via chemical reduction of exfoliated graphite oxide, *Carbon* 45 (2007) 1558–1565.
- [4] K.S. Kim, Y. Zhao, H. Jang, S.Y. Lee, J.M. Kim, K.S. Kim, J.-H. Ahn, P. Kim, J.-Y. Choi, B.H. Hong, Large-scale pattern growth of graphene films for stretchable transparent electrodes, *Nature* 457 (2009) 706–710.
- [5] A. Reina, X. Jia, J. Ho, D. Nezich, H. Son, V. Bulovic, M.S. Dresselhaus, J. Kong, Few-layer graphene films on arbitrary substrates by chemical vapor deposition, *Nano Lett.* 9 (2009) 30–35.
- [6] O.M. Istrate, K.R. Paton, U. Khan, A. O'Neill, A.P. Bell, J.N. Coleman, Reinforcement in melt-processed polymer-graphene composites at extremely low graphene loading level, *Carbon* 78 (2014) 243–249.
- [7] J.M. Garcia, Rui He, Mason P. Jiang, Jun Yan, Aron Pinczuk, Yuri M. Zuev, KeunSoo Kim, Philip Kim, Kirk Baldwin, Ken W. West, Loren N. Pfeiffer, Multilayer graphene films grown by molecular beam deposition, *Solid State Commun.* 150 (2010) 809–811.
- [8] J.M. Garcia, U. Wurstbauer, A. Levy, L.N. Pfeiffer, A. Pinczuk, A.S. Plaut, L. Wang, C.R. Dean, R. Buizza, A.M. Van Der Zande, J. Hone, K. Watanabe, T. Taniguchi, Graphene growth on h-BN by molecular beam epitaxy, *Solid State Commun.* 152 (2012) 975–978.
- [9] A.J. Martinez-Galera, I. Brihuega, J.M. Gomez-Rodriguez, Ethylene irradiation: a new route to grow graphene on low reactivity metals, *Nano Lett.* 11 (2011) 3576–3580.
- [10] G. Otero, C. Gonzalez, A.L. Pinardi, P. Merino, S. Gardonio, S. Lizzit, M. Blanco-Rey, K. Van de Ruit, C.F.J. Flipse, J. Mendez, P.L. de Andres, J.A. Martin-Gago, Ordered Vacancy Network Induced by the Growth of Epitaxial Graphene on Pt(111), *Physical Review Letters* 105, 2010.
- [11] S. Nie, N.C. Bartelt, J.M. Wofford, O.D. Dubon, K.F. McCarty, K. Thuermer, Scanning tunneling microscopy study of graphene on Au(111): growth mechanisms and substrate interactions, *Phys. Rev. B* 85 (2012).
- [12] B. Kiraly, E.V. Iski, A.J. Mannix, B.L. Fisher, M.C. Hersam, N.P. Guisinger, Solid-source growth and atomic-scale characterization of graphene on Ag(111), *Nat. Commun.* 4 (2013).
- [13] Meng-Yu Lin, Wei-Ching Guo, Wu. Meng-Hsun, Pro-Yao Wang, Te-Huan Liu, Chun-Wei Pao, Chien-Cheng Chang, Si-Chen Lee, Shih-Yen Lin, Low-temperature grown graphene films by using molecular beam epitaxy, *Appl. Phys. Lett.* 101 (2012) 221911.
- [14] S.-K. Jerng, D.S. Yu, J.H. Lee, C. Kim, S. Yoon, S.-H. Chun, Graphitic carbon growth on crystalline and amorphous oxide substrates using molecular beam epitaxy, *Nano-scale Res. Lett.* 6 (2011).
- [15] E. Loginova, N.C. Bartelt, P.J. Feibelman, K.F. McCarty, Evidence for graphene growth by C cluster attachment, *New J. Phys.* 10 (2008).
- [16] E. Moreau, S. Godey, F.J. Ferrer, D. Vignaud, X. Wallart, J. Avila, M.C. Asensio, F. Bournel, J.J. Gallet, Graphene growth by molecular beam epitaxy on the carbon-face of SiC, *Appl. Phys. Lett.* 97 (2010).



- [17] J. Park, W.C. Mitchel, L. Grazulis, H.E. Smith, K.G. Eyink, J.J. Boeckl, D.H. Tomich, S.D. Pacey, J.E. Hoelscher, Epitaxial graphene growth by carbon molecular beam epitaxy (CMBE), *Adv. Mater.* 22 (2010) 4140–+.
- [18] U. Wurstbauer, T. Schiros, C. Jaye, A.S. Plaut, R. He, A. Rigosi, C. Gutierrez, D. Fischer, L.N. Pfeiffer, A.N. Pasupathy, A. Pinczuk, J.M. Garcia, Molecular beam growth of graphene nanocrystals on dielectric substrates, *Carbon* 50 (2012) 4822–4829.
- [19] F. Viñes, K.M. Neyman, A. Goerling, Carbon on platinum substrates: from carbidic to graphitic phases on the (111) surface and on nanoparticles, *J. Phys. Chem. A* 113 (2009) 11963–11973.
- [20] I. Horcas, R. Fernandez, J.M. Gomez-Rodriguez, J. Colchero, J. Gomez-Herrero, A.M. Baro, WSXM: a software for scanning probe microscopy and a tool for nanotechnology, *Rev. Sci. Instrum.* 78 (2007).
- [21] P. Merino, M. Svec, A.L. Pinardi, G. Otero, J.A. Martin-Gago, Strain-driven moire superstructures of epitaxial graphene on transition metal surfaces, *AcsNano* 5 (2011) 5627–5634.
- [22] M. Gao, Y. Pan, L. Huang, H. Hu, L.Z. Zhang, H.M. Guo, S.X. Du, H.J. Gao, Epitaxial growth and structural property of graphene on Pt(111), *Appl. Phys. Lett.* 98 (2011).
- [23] P. Sutter, J.T. Sadowski, E. Sutter, Graphene on Pt(111): growth and substrate interaction, *Phys. Rev. B* 80 (2009).
- [24] T.A. Land, T. Michely, R.J. Behm, J.C. Hemminger, G. Comsa, STM investigation of single layer graphite structures produced on Pt(111) by hydrocarbon decomposition, *Surf. Sci.* 264 (1992) 261–270.
- [25] J.M. Wofford, E. Starodub, A.L. Walter, S. Nie, A. Bostwick, N.C. Bartelt, K. Thurmer, E. Rotenberg, K.F. McCarty, O.D. Dubon, Extraordinary epitaxial alignment of graphene islands on Au(111), *New J. Phys.* 14 (2012).
- [26] J.M. Blanco, C. González, P. Jelinek, J. Ortega, F. Flores, R. Pérez, M. Rose, M. Salmerón, J. Méndez, J. Wintterlin, G. Ertl, Origin of contrast in STM images of oxygen on Pd(111) and its dependence on tip structure and tunneling parameters, *Phys. Rev. B* 71 (2005) 113402.
- [27] N. Nicoara, E. Roman, J.M. Gomez-Rodriguez, J.A. Martin-Gago, J. Mendez, Scanning tunneling and photoemission spectroscopies at the PTCD/Au(111) interface, *Org. Electron.* 7 (2006) 287–294.
- [28] We have used ab-initio Density Functional Theory to get diffusion barriers for carbon on gold (0.825 eV) and on platinum (0.886 eV). A model consisting of four  $2 \times 2$  fcc (111) layers has been used. Ultra-soft pseudopotentials (300 eV cutoff), a  $4 \times 4 \times 1$  k-mesh, and PBE for exchange and correlation has been used. Calculations have been performed with CASTEP [29] using a Linear Synchronous Transit Method to locate the transition state. At 832 K, carbon atoms on gold jumps need about 100 ns to jump from one cell to a neighboring one. That same rate can be obtained on platinum by increasing the temperature to 893 K.
- [29] S.J. Clark, M.D. Segall, C.J. Pickard, P.J. Hasnip, M.J. Probert, K. Refson, M.C. Payne, First principles methods using CASTEP, *Z. Kristallogr.* 220 (2005) 567–570.